Journal of Computational and Applied Mathematics 367 (2020) 112420

Contents lists available at ScienceDirect

Journal of Computational and Applied Mathematics

journal homepage: www.elsevier.com/locate/cam

Preconditioned modified Hermitian and skew-Hermitian splitting iteration methods for fractional nonlinear Schrödinger equations

Zeng-Qi Wang [a,1], Jun-Feng Yin [b,*], Quan-Yu Dou [b]

[a] School of Mathematical Sciences, Shanghai Jiaotong University, Shanghai, 200240, PR China
[b] School of Mathematical Sciences, Tongji University, Shanghai, 200092, PR China

ARTICLE INFO

Article history:
Received 7 January 2018
Received in revised form 5 July 2019

Keywords:
The space fractional Schrödinger equations
Toeplitz matrix
HSS iteration methods
Convergence analysis
Preconditioning

ABSTRACT

A variant of preconditioned modified Hermitian and skew-Hermitian splitting (PMHSS) iteration method is proposed for a class of Toeplitz-like complex linear equations arising from the space fractional coupled nonlinear Schrödinger equations. Theoretical analysis show that the new method is convergent unconditionally. Moreover, the choice of the theoretical optimal parameter is further studied in detail, which minimize the upper bound of the spectral radius and relate to the extreme eigenvalues of the Toeplitz matrix and the extreme absolute values of the diagonal matrix. In addition, the splitting can be used as a preconditioner for Krylov subspaces method. Numerical experiments show that the proposed method is efficient, and the optimal parameter is independent of the mesh size which is very useful in large sparse practical problem.

1. Introduction

The Schrödinger equation is one of the most important equations of quantum physics for describing nonrelativistic quantum mechanical behavior. Feynman and Hibbs derived the standard Schrödinger equation from the path integrals over Brownian paths. A natural generalization of the Brownian motion is Lévy stochastic process. Recently, Laskin [1] derived the space fractional Schrödinger equation by extending the Feynman path integral to Lévy one, which contains the standard Schrödinger equation as its special case.

The fractional partial differential equations can describe some real physical phenomena better than integral partial differential equations, especially in optics and hydrodynamics. Guo and Xu [2] discussed the physical applications of fractional Schrödinger equation and obtained the exact solutions with several kinds of potentials. Guo, Han and Xin [3] proved the existence of the global smooth solution of fractional nonlinear Schrödinger equation with periodic boundary conditions. Hu, Xin and Lu [4] further studied the existence and uniqueness of the global solution of fractional coupled nonlinear Schrödinger equations.

However, the exact solutions of fractional differential equations often contain some special functions, such as Fox functions, which are still not easily to simulate. The numerical methods for fractional differential equations become important tools to understand the behaviors of the equations [5,6]. A number of numerical methods including the finite difference methods [7–9], pseudo-spectral methods [10], and multi-symplectic methods [11,12] are developed

* Corresponding author.
E-mail addresses: wangzengqi@sjtu.edu.cn (Z.-Q. Wang), yinjf@tongji.edu.cn (J.-F. Yin), 08douquanyu@tongji.edu.cn (Q.-Y. Dou).

[1] This work is supported by the National Natural Science Foundation of China under Grant No. 11971354.

https://doi.org/10.1016/j.cam.2019.112420
0377-0427/

for discretizing the nonlinear Schrödinger equations. For instances, Wang, Xiao and Yang [8,9] discussed the stability and convergence of some difference schemes for coupled nonlinear Schrödinger equations. Sun and Zhao [13] studied a second-order-convergent conservative difference scheme in L_∞ norm.

In this paper, we consider the following coupled nonlinear Schrödinger equations

$$\begin{cases} iu_t + \gamma(-\Delta)^{\alpha/2}u + \rho(|u|^2 + \beta|v|^2)u &= 0, \\ iv_t + \gamma(-\Delta)^{\alpha/2}v + \rho(|v|^2 + \beta|u|^2)v &= 0. \end{cases} \quad a \le x \le b, 0 < t \le T \tag{1.1}$$

with the initial boundary value conditions

$$\begin{cases} u(x,0) = u_0(x), & v(x,0) = v_0(x), & a \le x \le b, \\ u(a,t) = u(b,t) = 0, & v(a,t) = v(b,t) = 0, & 0 \le t \le T. \end{cases}$$

where $\mathrm{i} = \sqrt{-1}$, $1 < \alpha < 2$ and the parameters $\gamma, \rho > 0$, $\beta \ge 0$ are constants. When $\alpha = 2$, the system (1.1) is reduced to the classical coupled nonlinear Schrödinger equations, which describe a wide class of physical nonlinear phenomena, such as the hydrodynamics, the nonlinear optics and the dynamics of the two-component Bose–Einstein condensate.

As the coefficient matrix of the discretized linear system is the sum of a complex scaled identity matrix, a diagonal matrix and a symmetric Toeplitz matrix, the fast algorithms such as fast Fourier transform (FFT) for Toeplitz matrix–vector multiplication, the fast solvers for the circulant linear system, could be fully taken into account for designing the effective and efficient iterative methods. In addition, the linear system is ill-conditioned so that it leads to the slow convergence of the Krylov subspace methods. Ng and Pan [14] proposed approximate inverse circulant-plus-diagonal preconditioners for solving Hermitian positive definite Toeplitz-plus-diagonal systems. They use circulant matrices to approximate the inverses of Toeplitz matrices and combine these circulant matrices together. Motivated by this idea, Lei and Sun [15] and Pan et al. [16] presented circulant preconditioners and approximate inverse preconditioners for diagonal-times-Toeplitz matrices in fractional diffusion equations. We refer to [17,18] and [19] for the efficient solvers and preconditioners for the Toeplitz-like systems. It is noted that the Hermitian and skew-Hermitian parts of the coefficient matrix are the diagonal-plus-Toeplitz matrix and the complex scaled identity matrix respectively, Ran, Wang and Wang [5] proposed the HSS-like iteration method as well as the corresponding preconditioning technique for the discretized linear system of (1.1) on the basis of Hermitian and skew-Hermitian splitting(HSS) method [20]. The primary computing in the methods is solving a complex diagonal linear system and a Toeplitz linear system which is performed by fast solver. Moreover, an inexact version of HSS-like method and a new preconditioner are studied in [6,21] respectively.

In order to avoid the complex value arithmetic, we transform the original complex linear system into its equivalent two-by-two block real linear system, then solve the real linear system by the preconditioned modified Hermitian and skew-Hermitian splitting iteration (PMHSS) method [22]. Theoretical analyses show the convergent performance of the proposed method. Moreover, the theoretical optimal parameter is analyzed in detail by minimizing an upper bound of the spectral radius of the iteration matrix. The numerical experiments show that the theoretical optimal parameter is very close to the interval containing the experimental optimal parameters. The convergence of PMHSS iteration method is very stable in the neighborhood of the optimal parameter. An important phenomenon is that the convergence of the proposed iterative scheme and the corresponding preconditioned GMRES method is independent of not only the discretizing mesh size but also the parameters in the fractional nonlinear Schrödinger equations.

This paper is organized as follows. The discretization of the fractional Schrödinger equations and the sequent complex Toeplitz-like linear system is briefly introduced in Section 2. The PMHSS iteration method and its optimal parameter are studied in Section 3 as well as the preconditioning technique. In Section 4, the numerical experiments are presented to demonstrate the efficiency of the proposed methods. Finally, conclusions are drawn in Section 5.

2. Discretization of the fractional Schrödinger equations

The fractional Laplacian operator in (1.1) can be characterized as

$$(-\Delta)^{\frac{\alpha}{2}}u(x,t) = \mathcal{F}^{-1}\left(|\xi|^\alpha \mathcal{F}(u(x,t))\right),$$

where $\mathcal{F}$ is the Fourier transform acting on the spatial variable x. Furthermore, it is shown that the Riesz fractional derivative can also be defined as

$$\frac{\partial^\alpha}{\partial|x|^\alpha}u(x,t) = -(-\Delta)^{\frac{\alpha}{2}}u(x,t) = -\frac{1}{2\cos\frac{\pi\alpha}{2}}\left[{}_{-\infty}D_x^\alpha u(x,t) + {}_xD_{+\infty}^\alpha u(x,t)\right],$$

where ${}_{-\infty}D_x^\alpha$ and ${}_xD_{+\infty}^\alpha$ are the left and right Riemann–Liouville derivatives, respectively.

Let M and N be the numbers of the discrete points in spatial and temporal dimensions respectively. Accordingly, denoted by $\tau = T/N$ and $h = (b-a)/(M+1)$ the temporal step size and the spatial step size, $t_n = n\tau$ for $n = 0, 1, \ldots, N$ and $x_j = a + jh$ for $j = 0, 1, \ldots, M+1$.

Let $u_j^n \approx u(x_j, t_n)$ and $v_j^n \approx v(x_j, t_n)$ denote the corresponding numerical solutions. The fractional Laplacian $(-\Delta)^{\frac{\alpha}{2}}$ is discreted by the fractional centered difference in the truncated bounded domain as

$$(-\Delta)^{\frac{\alpha}{2}}u(x_j,t) = -\frac{\partial^\alpha}{\partial|x|^\alpha}u(x_j,t) = \frac{1}{h^\alpha}\sum_{k=1}^{M} c_{j-k}u_k + \mathcal{O}(h^2),$$

where the coefficient

$$c_k = \frac{(-1)^k \Gamma(\alpha+1)}{\Gamma(\alpha/2-k+1)\Gamma(\alpha/2+k+1)},$$

with $\Gamma(\cdot)$ being the gamma function. The coefficients c_k satisfy the following properties

$$\begin{cases} c_0 \geq 0, \\ c_k = c_{-k} \leq 0, k = 1, 2, \ldots, \\ \sum_{k=-\infty, k\neq 0}^{+\infty} |c_k| = c_0. \end{cases}$$

By applying the linearly implicit difference scheme proposed in [8], the following discretized scheme of the space fractional coupled nonlinear Schrödinger equations (1.1) is obtained

$$\begin{cases} i\frac{u_j^{n+1}-u_j^{n-1}}{2\tau} + \frac{\gamma}{h^\alpha}\sum_{k=1}^{M} c_{j-k}\hat{u}_j^n + \rho(|u_j^n|^2 + \beta|v_j^n|^2)\hat{u}_j^n = 0, \\ i\frac{v_j^{n+1}-v_j^{n-1}}{2\tau} + \frac{\gamma}{h^\alpha}\sum_{k=1}^{M} c_{j-k}\hat{v}_j^n + \rho(|v_j^n|^2 + \beta|u_j^n|^2)\hat{v}_j^n = 0, \end{cases} \tag{2.1}$$

where $\hat{u}_j^n = \frac{u_j^{n+1}+u_j^{n-1}}{2}$, $\hat{v}_j^n = \frac{v_j^{n+1}+v_j^{n-1}}{2}$, $j = 1, 2, \ldots, M$, $n = 1, 2, \ldots, N-1$. It is proved that the scheme (2.1) conserves the discrete mass and energy, and is unconditional stable and convergent with order $\mathcal{O}(\tau^2 + h^2)$ in the discrete l^2 norm [8,9].

By the initial boundary value conditions, we have

$$u_j^0 = u_0(x_j),\ v_j^0 = v_0(x_j),\ j = 1, 2, \ldots, M,$$

and

$$u_0^n = u_{M+1}^n = 0,\ v_0^n = v_{M+1}^n = 0,\ n = 1, 2, \ldots, N.$$

In addition, the first step can be obtained by some second or higher order temporal integrators. The two difference equations in (2.1) have the same algebraic structure. Denote $u^{n+1} = [u_1^{n+1}, \ldots, u_M^{n+1}]^T$ and $b^{n+1} = [b_1^{n+1}, \ldots, b_M^{n+1}]^T$, where

$$b_j^{n+1} = \mathrm{i}b_j^{n-1} - \mu\sum_{k=1}^{M} c_{j-k}u_k^{n-1} - d_j^{n+1}u_j^{n-1},\ j = 1, 2, \ldots, M,$$

with

$$\mu = \frac{\gamma\tau}{h^\alpha}, \quad \text{and} \quad d_j^{n+1} = \rho\tau(|u_j^n|^2 + \beta|v_j^n|^2).$$

Consequently, the first difference scheme in (2.1) is rewritten as

$$A^{n+1}u^{n+1} = b^{n+1},\ n = 1, 2, \ldots, N-1, \tag{2.2}$$

where the coefficient matrix is of the form

$$A^{n+1} = \mathrm{i}I + D^{n+1} + T.$$

Here, I is the identity matrix, D^{n+1} is the nonnegative diagonal matrix defined by

$$D^{n+1} = \mathrm{diag}(d_1^{n+1}, d_2^{n+1}, \ldots, d_M^{n+1}),$$

and T is the Toeplitz matrix

$$T = \mu\begin{pmatrix} c_0 & c_1 & \vdots & c_{2-M} & c_{1-M} \\ c_{-1} & c_0 & \vdots & c_{3-M} & c_{2-M} \\ \vdots & \vdots & \ddots & \vdots & \vdots \\ c_{M-2} & c_{M-3} & \vdots & c_0 & c_1 \\ c_{M-1} & c_{M-2} & \vdots & c_{-1} & c_0 \end{pmatrix}. \tag{2.3}$$

From the facts that $\gamma, \rho > 0$, $\beta \geq 0$ and the properties of the coefficients c_k, it is seen that the Toeplitz matrix T is symmetric and strictly diagonally dominant, hence symmetric positive definite. Thus, the matrix $D^{n+1} + T$ is symmetric positive definite, which results in the fact that the coefficient matrix A^{n+1} is complex symmetric and non-Hermitian positive definite. It is clear that the second equation in (2.1) could be written as a complex linear system in the same way. The coefficient matrix has the same structure as A^{n+1} in (2.2).

3. Preconditioned modified HSS iteration method and preconditioning

In this section, we consider the iteration method and preconditioners for the complex linear systems of equations in the form of

$$Au = b, \tag{3.1}$$

where $A = D + T + \mathrm{i}I$ is a Toeplitz like matrix, with $D \in \mathbb{R}^{n\times n}$ a positive diagonal matrix and $T \in \mathbb{R}^{n\times n}$ a symmetric positive definite Toeplitz matrix; $u = y + \mathrm{i}z$ and $b = p + \mathrm{i}q$ are complex vectors while y, z, p, q are real vectors in $\mathbb{R}^n$. (2.2). The symmetric complex linear system could be transformed into the following real two-by-two block linear system equivalently

$$Rx \equiv \begin{pmatrix} \mathbf{W} & -\mathbf{T} \\ \mathbf{T} & \mathbf{W} \end{pmatrix} \begin{pmatrix} y \\ z \end{pmatrix} = \begin{pmatrix} p \\ q \end{pmatrix} \equiv g, \tag{3.2}$$

where $\mathbf{W} = D + T$ is its real part and $\mathbf{T} = I$ is its imaginary part. $\mathbf{W}$ is a symmetric Toeplitz-plus-diagonal matrix since T is a symmetric Toeplitz matrix and D is a diagonal matrix. The PMHSS iteration method [22,23] is proved to be a very efficient iterative method for solving (3.2). It is stated as follows:

Method 3.1 (*PMHSS Iteration Method for Solving* (3.2))**.** *Let $(y^{(0)^T}, z^{(0)^T}) \in \mathbb{R}^n$ be an arbitrary initial guess. For $k = 0, 1, 2, \ldots$, until the sequence of iterates $\{(y^{(k)^T}, z^{(k)^T})\}_{k=0}^{\infty} \subset \mathbb{R}^n$ converges, compute the next iterate $(y^{(k+1)^T}, z^{(k+1)^T})$ according to the following procedure:*

$$\begin{cases} \begin{pmatrix} \alpha\mathbf{V}+\mathbf{W} & 0 \\ 0 & \alpha\mathbf{V}+\mathbf{W} \end{pmatrix} \begin{pmatrix} y^{(k+1/2)} \\ z^{(k+1/2)} \end{pmatrix} = \begin{pmatrix} \alpha\mathbf{V} & \mathbf{T} \\ -\mathbf{T} & \alpha\mathbf{V} \end{pmatrix} \begin{pmatrix} y^{(k)} \\ z^{(k)} \end{pmatrix} + \begin{pmatrix} p \\ q \end{pmatrix}, \\ \begin{pmatrix} \alpha\mathbf{V}+\mathbf{T} & 0 \\ 0 & \alpha\mathbf{V}+\mathbf{T} \end{pmatrix} \begin{pmatrix} y^{(k+1)} \\ z^{(k+1)} \end{pmatrix} = \begin{pmatrix} \alpha\mathbf{V} & -\mathbf{W} \\ \mathbf{W} & \alpha\mathbf{V} \end{pmatrix} \begin{pmatrix} y^{(k+1/2)} \\ z^{(k+1/2)} \end{pmatrix} + \begin{pmatrix} q \\ -p \end{pmatrix}. \end{cases}$$

where α is a positive parameter and $\mathbf{V}$ is a symmetric positive definite matrix.

To take full advantage of the Toeplitz matrix, we take $\alpha\mathbf{V} = \omega I - D$. Denote the diagonal elements of D by $d_i, i = 1, \ldots, n$. Then $\omega > \max_i |d_i|$, so that $\omega I - D$ is positive definite. Then, we get the PMHSS iteration scheme for solving linear system (3.2) as follows:

Method 3.2 (*The Special Case of the PMHSS Iteration Method*)**.** *Let $(y^{(0)^T}, z^{(0)^T}) \in \mathbb{R}^n$ be an arbitrary initial guess. For $k = 0, 1, 2, \ldots$, until the sequence of iterates $\{(y^{(k)^T}, z^{(k)^T})\}_{k=0}^{\infty} \subset \mathbb{R}^n$ converges, compute the next iterate $(y^{(k+1)^T}, z^{(k+1)^T})$ according to the following procedure:*

$$\begin{cases} \begin{pmatrix} \omega I + T & 0 \\ 0 & \omega I + T \end{pmatrix} \begin{pmatrix} y^{(k+1/2)} \\ z^{(k+1/2)} \end{pmatrix} = \begin{pmatrix} \omega I - D & I \\ -I & \omega I - D \end{pmatrix} \begin{pmatrix} y^{(k)} \\ z^{(k)} \end{pmatrix} + \begin{pmatrix} p \\ q \end{pmatrix} \\ \begin{pmatrix} (\omega+1)I - D & 0 \\ 0 & (\omega+1)I - D \end{pmatrix} \begin{pmatrix} y^{(k+1)} \\ z^{(k+1)} \end{pmatrix} = \begin{pmatrix} \omega I - D & -D - T \\ D + T & \omega I - D \end{pmatrix} \begin{pmatrix} y^{(k+1/2)} \\ z^{(k+1/2)} \end{pmatrix} + \begin{pmatrix} q \\ -p \end{pmatrix} \end{cases}$$

In every iteration step, the primary computing is solving two Toeplitz linear systems of $\omega I + T$ and two diagonal linear systems $(\omega + 1)I - D$. The method is considerable efficient since the Toeplitz systems could be solved by fast solvers.

The PMHSS sequence generates in Method 3.2 could be reformulated as

$$x^{(k+1)} = \mathbf{L}(\omega)x^{(k)} + \mathbf{F}^{-1}(\omega)g,$$

with $x^{(k)} = (y^{(k)^T},\ z^{(k)^T})^T$, $g = (p^T, q^T)^T$,

$$\mathbf{L}(\omega) = \begin{pmatrix} (\omega+1)I - D & 0 \\ 0 & (\omega+1)I - D \end{pmatrix}^{-1} \begin{pmatrix} \omega I - D & -D - T \\ D + T & \omega I - D \end{pmatrix} \cdot \begin{pmatrix} \omega I + T & 0 \\ 0 & \omega I + T \end{pmatrix}^{-1} \begin{pmatrix} \omega I - D & I \\ -I & \omega I - D \end{pmatrix},$$

and

$$\mathbf{F}^{-1}(\omega) = \begin{pmatrix} (\omega+1)I - D & 0 \\ 0 & (\omega+1)I - D \end{pmatrix}^{-1} \cdot \left[\begin{pmatrix} 0 & I \\ -I & 0 \end{pmatrix} + \begin{pmatrix} \omega I - D & -D - T \\ D + T & \omega I - D \end{pmatrix} \begin{pmatrix} \omega I + T & 0 \\ 0 & \omega I + T \end{pmatrix}^{-1} \right]$$

$$= \begin{pmatrix} (\omega+1)I - D & 0 \\ 0 & (\omega+1)I - D \end{pmatrix}^{-1} \begin{pmatrix} \omega I - D & \omega I - D \\ -\omega I + D & \omega I - D \end{pmatrix} \begin{pmatrix} \omega I + T & 0 \\ 0 & \omega I + T \end{pmatrix}^{-1}$$

$$= (\omega I + T)^{-1}(\omega I - D)(\omega I + T)^{-1} \begin{pmatrix} I & I \\ -I & I \end{pmatrix}.$$

Thus, it is obtained that

$$\mathbf{F}(\omega) = \frac{1}{2} \begin{pmatrix} I & -I \\ I & I \end{pmatrix} (\omega I + T)^{-1}(\omega I - D)(\omega I + T)^{-1}.$$

Actually, the PMHSS iteration method in Method 3.2 implies a matrix splitting as follows

$$R = \mathbf{F}(\omega) - \mathbf{G}(\omega), \tag{3.3}$$

where

$$\mathbf{G}(\omega) = \frac{1}{2}(\omega I - D)^{-1} \begin{pmatrix} I & -I \\ I & I \end{pmatrix} \begin{pmatrix} \omega I - D & -(D+T) \\ D+T & \omega I - D \end{pmatrix} \begin{pmatrix} \omega I - D & I \\ -I & \omega I - D \end{pmatrix}.$$

so that the iteration matrix $\mathbf{L}(\omega)$ can be denoted by $\mathbf{F}(\omega)^{-1}\mathbf{G}(\omega)$.

We should point out that the splitting matrix $F(\omega)$ plays an important role in the PMHSS iteration method and can be served as the preconditioner for the Krylov subspace method. We call it PMHSS preconditioner in the following page. In actual implementations, the action of the preconditioning is solving a sequence of generalized residual equations

$$\mathbf{F}(\omega)z^{(k)} = r^{(k)},$$

where $r^{(k)}$ is a current residual vector. Therefore, the primary cost is solving two diagonal linear systems with $(\omega+1)I - D$ and two linear systems with $\omega I + T$. Since $\omega I + T$ is a Toeplitz matrix, it could be solved by the fast solvers introduced by [17–19,24].

According to Theorem 2.1 in [23], the sequence generated by Method 3.2 converges to the unique solution when $\omega I - D$ is symmetric positive, which is equivalent to $\omega > \max_{1\le i\le n}\{d_i\}$.

Denote $\mathbf{K}_1 = (\omega I - D)^{-1/2}(D+T)(\omega I - D)^{-1/2}$ and $\mathbf{K}_2 = (\omega I - D)^{-1}$, it follows that

$$\begin{aligned}
\mathbf{L}(\omega) = & \begin{pmatrix} \omega I - D + I & 0 \\ 0 & \omega I - D + I \end{pmatrix}^{-1} \begin{pmatrix} \omega I - D & -(D+T) \\ D+T & \omega I - D \end{pmatrix} \\
& \cdot \begin{pmatrix} \omega I + T & 0 \\ 0 & \omega I + T \end{pmatrix}^{-1} \begin{pmatrix} \omega I - D & I \\ -I & \omega I - D \end{pmatrix} \\
\backsim & \begin{pmatrix} \omega I - D & -(D+T) \\ D+T & \omega I - D \end{pmatrix} \begin{pmatrix} \omega I + T & 0 \\ 0 & \omega I + T \end{pmatrix}^{-1} \\
& \cdot \begin{pmatrix} \omega I - D & I \\ -I & \omega I - D \end{pmatrix} \begin{pmatrix} \omega I - D + I & 0 \\ 0 & \omega I - D + I \end{pmatrix}^{-1} \\
\backsim & \begin{pmatrix} I & -\mathbf{K}_1 \\ \mathbf{K}_1 & I \end{pmatrix} \begin{pmatrix} I + \mathbf{K}_1 & 0 \\ 0 & I + \mathbf{K}_1 \end{pmatrix}^{-1} \\
& \cdot \begin{pmatrix} I & \mathbf{K}_2 \\ -\mathbf{K}_2 & I \end{pmatrix} \begin{pmatrix} I + \mathbf{K}_2 & 0 \\ 0 & I + \mathbf{K}_2 \end{pmatrix}^{-1},
\end{aligned}$$

and thus

$$\rho(\mathbf{L}(\omega)) \le \| \begin{pmatrix} I & -\mathbf{K}_1 \\ \mathbf{K}_1 & I \end{pmatrix} \begin{pmatrix} I + \mathbf{K}_1 & 0 \\ 0 & I + \mathbf{K}_1 \end{pmatrix}^{-1} \| \| \begin{pmatrix} I & \mathbf{K}_2 \\ -\mathbf{K}_2 & I \end{pmatrix} \begin{pmatrix} I + \mathbf{K}_2 & 0 \\ 0 & I + \mathbf{K}_2 \end{pmatrix}^{-1} \|.$$

Taking the 2-norm of the matrix, we obtain the upper bound of spectral radius of $\mathbf{L}(\omega)$ as follows:

$$\sigma(\omega) \equiv \max_{1\le j\le n} \frac{\sqrt{1+\lambda_j^2}}{1+\lambda_j} \cdot \max_{1\le j\le n} \frac{\sqrt{1+\mu_j^2}}{1+\mu_j}. \tag{3.4}$$

Here, λ_j and μ_j, $j = 1, \ldots, n$, are the eigenvalues of $(\omega I - D)^{-1}(D+T)$ and $(\omega I - D)^{-1}$, respectively.

Let ξ be the eigenvector corresponding to the eigenvalue λ_j and satisfy

$$(\omega I - D)^{-1}(D+T)\xi = \lambda_j \xi.$$

Consequently, we obtain

$$\lambda_j = \frac{\frac{\xi^* D\xi}{\xi^*\xi} + \frac{\xi^* T\xi}{\xi^*\xi}}{\omega - \frac{\xi^* D\xi}{\xi^*\xi}},$$

which is lower and upper bounded by

$$\lambda_{\min} = \frac{d_n + \tau_n}{\omega - d_n} \le \lambda_j \le \frac{d_1 + \tau_1}{\omega - d_1} = \lambda_{\max}, \quad j = 1, \ldots, n,$$

where τ_1 and τ_n are the largest and smallest eigenvalues of Toeplitz matrix T, d_1 and d_n are the largest and smallest elements of diagonal matrix D, respectively. Similarly, μ_j lower and upper bounded by

$$\mu_{\min} = \frac{1}{\omega - d_n} \le \mu_j \le \frac{1}{\omega - d_1} = \mu_{\max}, \quad j = 1, \ldots, n.$$

We define the functions $f(x) = \frac{\sqrt{1+x^2}}{1+x}$ with $x \in \mathbb{R}^+$ and

$$\sigma(\lambda, \mu) \equiv f(\lambda) f(\mu) = \frac{\sqrt{1+\lambda^2}}{1+\lambda} \cdot \frac{\sqrt{1+\mu^2}}{1+\mu},$$

with $\lambda \in [\lambda_{\min},\ \lambda_{\max}]$ and $\mu \in [\mu_{\min},\ \mu_{\max}]$. It is clear that

$$\rho(L(\omega)) \le \sigma(\omega) \le \hat{\sigma}(\omega),$$

where

$$\hat{\sigma}(\omega) = \max_{\lambda \in [\lambda_{\min},\ \lambda_{\max}]} \max_{\mu \in [\mu_{\min},\ \mu_{\max}]} \sigma(\omega, \lambda, \mu).$$

In the following, instead of analyzing the optimal parameter ω to minimize the spectral radius of $L(\omega)$, we are looking for the optimal parameter ω for the following continuous optimization problems:

$$\min_{\omega \in (d_1,\ \infty)} \hat{\sigma}(\omega).$$

It is clear that $f(x)$ is a decreasing function when $x \le 1$ and increasing function when $x \ge 1$. It reaches its minimum at $x = 1$. Therefore,

$$\max_{\lambda \in [\lambda_{\min},\ \lambda_{\max}]} f(\lambda) = \begin{cases} f(\lambda_{\max}), & \text{when } d_1 < \omega < \omega_1; \\ f(\lambda_{\min}), & \text{when } \omega_1 \le \omega, \end{cases}$$

where $\omega_1 = \frac{1}{2}(d_1 + d_n) + \frac{1}{2}\sqrt{(d_1 + d_n)^2 + 4(d_1\tau_n + d_n\tau_1) + 4\tau_1\tau_n}$, and

$$\max_{\mu \in [\mu_{\min},\ \mu_{\max}]} f(\mu) = \begin{cases} f(\mu_{\max}), & \text{when } d_1 < \omega < \omega_2; \\ f(\mu_{\min}), & \text{when } \omega_2 \le \omega, \end{cases}$$

where $\omega_2 = \frac{1}{2}(d_1 + d_n + \sqrt{(d_1 + d_n)^2 + 4})$. By straightforward calculation, we obtain

$$\begin{cases} \omega_1 > \omega_2, & \text{if } \ d_n\tau_1 + d_1\tau_n + \tau_n\tau_1 - 1 > 0; \\ \omega_1 \le \omega_2, & \text{if } \ d_n\tau_1 + d_1\tau_n + \tau_n\tau_1 - 1 \le 0. \end{cases}$$

Therefore, we show the explicit expression of $\hat{\sigma}(\omega)$ in the following theorem.

Theorem 3.1. *Let A be a complex symmetric matrix defined as in (3.1) with D and T being positive diagonal matrix and symmetric positive definite Toeplitz matrix respectively. Denote that τ_1 and τ_n are the largest and smallest eigenvalues of matrix T, d_1 and d_n are the largest and smallest elements of matrix D respectively, and let $\omega > d_1$ be a positive parameter. The PMHSS iteration converges to the unique solution of the block two-by-two linear system for any initial guess, for the spectral radius of iterative matrix $\mathbf{L}(\omega)$ is bounded by*

$$\rho(\mathbf{L}(\omega)) \le \sigma(\omega) \le \hat{\sigma}(\omega) < 1,$$

where the upper bound $\hat{\sigma}(\omega)$ has piecewise definition:

(a) When $d_n\tau_1 + d_1\tau_n + \tau_n\tau_1 - 1 > 0$,

$$\hat{\sigma}(\omega) = \begin{cases} \dfrac{\sqrt{(\omega - d_1)^2 + (d_1 + \tau_1)^2}}{\omega + \tau_1} \dfrac{\sqrt{(\omega - d_1)^2 + 1}}{\omega - d_1 + 1}, & \text{when } \omega \le \omega_2; \\ \dfrac{\sqrt{(\omega - d_1)^2 + (d_1 + \tau_1)^2}}{\omega + \tau_1} \dfrac{\sqrt{(\omega - d_n)^2 + 1}}{\omega - d_n + 1}, & \text{when } \omega_2 \le \omega \le \omega_1; \\ \dfrac{\sqrt{(\omega - d_n)^2 + (d_n + \tau_n)^2}}{\omega + \tau_n} \dfrac{\sqrt{(\omega - d_n)^2 + 1}}{\omega - d_n + 1} & \text{when } \omega \ge \omega_1. \end{cases}$$

It obtains its minimum at

$$\omega_{\text{opt}} = \arg\min_{i=1,2,3} \hat{\sigma}(\omega_i),$$

with ω_3 is a solution of a quartic equation and also the minimum point in $[\omega_2,\ \omega_1]$;

(b) *When $d_n\tau_1 + d_1\tau_n + \tau_n\tau_1 - 1 \le 0$,*

$$\hat{\sigma}(\omega) = \begin{cases} \dfrac{\sqrt{(\omega-d_1)^2+(d_1+\tau_1)^2}}{\omega+\tau_1}\dfrac{\sqrt{(\omega-d_1)^2+1}}{\omega-d_1+1}, & \text{when } \omega \le \omega_1; \\ \dfrac{\sqrt{(\omega-d_n)^2+(d_n+\tau_n)^2}}{\omega+\tau_n}\dfrac{\sqrt{(\omega-d_1)^2+1}}{\omega-d_1+1}, & \text{when } \omega_1 \le \omega \le \omega_2; \\ \dfrac{\sqrt{(\omega-d_n)^2+(d_n+\tau_n)^2}}{\omega+\tau_n}\dfrac{\sqrt{(\omega-d_n)^2+1}}{\omega-d_n+1} & \text{when } \omega \ge \omega_2. \end{cases}$$

It obtains its minimum at

$$\omega_{\text{opt}} = \arg\min_{i=1,2,3} \hat{\sigma}(\omega_i),$$

with ω_3 is a solution of a quartic equation and also a minimum point in $[\omega_1,\ \omega_2]$.

Proof. We analyze $\hat{\sigma}(\omega)$ with several differentiated cases:

(a) When $d_n\tau_1 + d_1\tau_n + \tau_n\tau_1 - 1 > 0$, then $\omega_1 > \omega_2$,

(a1) In the case of $\omega \le \omega_2$,

$$\hat{\sigma}(\omega) = f(\lambda_{\max})f(\mu_{\max}) = \frac{\sqrt{(\omega-d_1)^2+(d_1+\tau_1)^2}}{\omega+\tau_1}\frac{\sqrt{(\omega-d_1)^2+1}}{\omega-d_1+1}.$$

Since $f(\lambda_{\max})$ and $f(\mu_{\max})$ are all monotonically decreasing functions with respect to ω, $\hat{\sigma}(\omega)$ gets its minimum at $\omega = \omega_2$, and

$$\hat{\sigma}(\omega_2) = f(\lambda_{\max})f(\mu_{\max}) = f(\frac{d_1+\tau_1}{\omega_2-d_1})f(\frac{1}{\omega_2-d_1});$$

(a2) In the case of $\omega_2 \le \omega \le \omega_1$,

$$\hat{\sigma}(\omega) = f(\lambda_{\max})f(\mu_{\min}) = \frac{\sqrt{(\omega-d_1)^2+(d_1+\tau_1)^2}}{\omega+\tau_1}\frac{\sqrt{(\omega-d_n)^2+1}}{\omega-d_n+1}.$$

It can be verified that $f(\lambda_{\max})$ is monotonically decreasing but $f(\mu_{\min})$ is monotonically increasing with respect to ω, respectively. The stationary points of $\hat{\sigma}(\omega)$, which satisfy $\dfrac{\partial\hat{\sigma}(\omega)}{\partial\omega} = 0$ are ought to be the solution of the following quartic equation:

$$a_0\omega^4 + a_1\omega^3 + a_2\omega^2 + a_3\omega + a_4 = 0, \tag{3.5}$$

where

$$\begin{aligned}
a_0 =\ & \tau_1 + d_1 + 1, \\
a_1 =\ & -\tau_1^2 + (-3d_1 - 3d_n + 2)\tau_1 - 2d_1^2 - 3d_1d_n - d_1 - d_n - 1, \\
a_2 =\ & 3d_n\tau_1^2 + (9d_1d_n + 3d_n^2 - 3d_1 - 3d_n)\tau_1 + 6d_1^2d_n + 3d_1d_n^2 + 3d_1, \\
a_3 =\ & \tau_1^3 + (-3d_n^2 + 2d_1 + d_n - 2)\tau_1^2 + (-9d_1d_n^2 - d_n^3 + 2d_1^2 + 6d_1d_n + d_n^2 - 3d_1 - d_n + 1)\tau_1 \\
& - 6d_1^2d_n^2 - d_1d_n^3 + 2d_1^2d_n + d_1d_n^2 - 4d_1^2 - d_1d_n + d_1, \\
a_4 =\ & (-d_n - 1)\tau_1^3 + (d_n^3 - 2d_1d_n - d_n^2 - 2d_1 + d_n - 1)\tau_1^2 \\
& + (3d_1d_n^3 - 2d_1^2d_n - 3d_1d_n^2 - 2d_1^2 + 3d_1d_n - 3d_1)\tau_1 \\
& + 2d_1^2d_n^3 - 2d_1^2d_n^2 + 2d_1^2d_n - 2d_1^2.
\end{aligned}$$

(a3) In the case of $\omega \ge \omega_1$,

$$\hat{\sigma}(\omega) = f(\lambda_{\min})f(\mu_{\min}) = \frac{\sqrt{(\omega-d_n)^2+(d_n+\tau_n)^2}}{\omega+\tau_n}\frac{\sqrt{(\omega-d_n)^2+1}}{\omega-d_n+1}.$$

since $f(\lambda_{\min})$ and $f(\mu_{\min})$ are all monotonically increasing with respect to ω, $\hat{\sigma}(\omega)$ gets its minimum at $\omega = \omega_1$, and

$$\hat{\sigma}(\omega_1) = f(\lambda_{\min})f(\mu_{\min}) = \frac{\sqrt{(\omega_1 - d_n)^2 + (d_n + \tau_n)^2}}{\omega_1 + \tau_n} \frac{\sqrt{(\omega_1 - d_n)^2 + 1}}{\omega_1 - d_n + 1}.$$

If Eq. (3.5) has solutions in the interval $[\omega_2,\ \omega_1]$, then we denote the one which has the minimized value of $\hat{\sigma}(\omega)$ as ω_3. then the optimal ω is the solution of

$$\omega_{\text{opt}} = \arg \min_{i=1,2,3} \hat{\sigma}(\omega_i);$$

If Eq. (3.5) has no solution in the interval $[\omega_2,\ \omega_1]$, the optimal ω is the solution of

$$\omega_{\text{opt}} = \arg \min_{i=1,2} \hat{\sigma}(\omega_i).$$

(b) When $d_n\tau_1 + d_1\tau_n + \tau_n\tau_1 - 1 < 0$, then $\omega_1 < \omega_2$. The analysis is similar with case (a).

(b1) In the case of $\omega \le \omega_1$,

$$\hat{\sigma}(\omega) = f(\lambda_{\max})f(\mu_{\max}) = \frac{\sqrt{(\omega - d_1)^2 + (d_1 + \tau_1)^2}}{\omega + \tau_1} \frac{\sqrt{(\omega - d_1)^2 + 1}}{\omega - d_1 + 1}.$$

Since $f(\lambda_{\max})$ and $f(\mu_{\max})$ are all monotonically decreasing functions with respect to ω, $\hat{\sigma}(\omega)$ gets its minimum at $\omega = \omega_1$, and

$$\hat{\sigma}(\omega_1) = f(\lambda_{\max})f(\mu_{\max}) = f(\frac{d_1 + \tau_1}{\omega_1 - d_1})f(\frac{1}{\omega_1 - d_1});$$

(b2) In the case of $\omega_1 < \omega < \omega_2$,

$$\hat{\sigma}(\omega) = f(\lambda_{\min})f(\mu_{\max}) = \frac{\sqrt{(\omega - d_n)^2 + (d_n + \tau_n)^2}}{\omega + \tau_n} \frac{\sqrt{(\omega - d_1)^2 + 1}}{\omega - d_1 + 1}.$$

It can be verified that $f(\lambda_{\max})$ is monotonically decreasing but $f(\mu_{\min})$ is monotonically increasing with respect to ω, respectively. The stationary points of $\hat{\sigma}(\omega)$, which satisfy $\frac{\partial \hat{\sigma}(\omega)}{\partial \omega} = 0$ are ought to be the solution of the following equation:

$$a_0\omega^4 + a_1\omega^3 + a_2\omega^2 + a_3\omega + a_4 = 0 \tag{3.6}$$

where

$$\begin{aligned}
a_0 = &\ \tau_n + d_n + 1,\\
a_1 = &\ -\tau_n^2 + (-3d_1 - 3d_n + 2)\tau_n - 3d_1d_n - 2d_n^2 - d_1 - d_n - 1,\\
a_2 = &\ 3d_1\tau_n^2 + (3d_1^2 + 9d_1d_n - 3d_1 - 3d_n)\tau_n + 3d_1^2d_n + 6d_1d_n^2 + 3d_n,\\
a_3 = &\ \tau_n^3 + (-3d_1^2 + d_1 + 2d_n - 2)\tau_n^2 + (-d_1^3 - 9d_1^2d_n + d_1^2 + 6d_1d_n + 2d_n^2 - d_1 - 3d_n + 1)\tau_n\\
&\ - d_1^3d_n - 6d_1^2d_n^2 + d_1^2d_n + 2d_1d_n^2 - d_1d_n - 4d_n^2 + d_n,\\
a_4 = &\ (-d_1 - 1)\tau_n^3 + (d_1^3 - d_1^2 - 2d_1d_n + d_1 - 2d_n - 1)\tau_n^2\\
&\ + (3d_1^3d_n - 3d_1^2d_n - 2d_1d_n^2 + 3d_1d_n - 2d_n^2 - 3d_n)\tau_n\\
&\ + 2d_1^3d_n^2 - 2d_1^2d_n^2 + 2d_1d_n^2 - 2d_n^2.
\end{aligned}$$

(b3) In the case of $\omega \le \omega_2$,

$$\sigma(\omega) = f(\lambda_{\min})f(\mu_{\min}) = \frac{\sqrt{(\omega - d_n)^2 + (d_n + \tau_n)^2}}{\omega + \tau_n} \frac{\sqrt{(\omega - d_n)^2 + 1}}{\omega - d_n + 1}$$

gets its minimum at $\omega = \omega_2$. since $f(\lambda_{\min})$ and $f(\mu_{\min})$ are all monotonically increasing with respect to ω, $\hat{\sigma}(\omega)$ gets its minimum at $\omega = \omega_2$, and

$$\hat{\sigma}(\omega_2) = f(\lambda_{\min})f(\mu_{\min}) = \frac{\sqrt{(\omega_2 - d_n)^2 + (d_n + \tau_n)^2}}{\omega_2 + \tau_n} \frac{\sqrt{(\omega_2 - d_n)^2 + 1}}{\omega_2 - d_n + 1}.$$

If Eq. (3.6) has solutions in $[\omega_1,\ \omega_2]$, then we denote the one which has the minimized value of $\hat{\sigma}(\omega)$ as ω_3. then the optimal ω is the solution of

$$\omega_{\text{opt}} = \arg \min_{i=1,2,3} \hat{\sigma}(\omega_i);$$

If Eq. (3.6) has no solution in $[\omega_1,\ \omega_2]$ the optimal ω is the solution of

$$\omega_{\text{opt}} = \arg\min_{i=1,2} \hat{\sigma}(\omega_i). \quad \blacksquare$$

We should give some remarks before going on for better understanding and making use of the optimal parameters in practical implementation.

Remark 3.1. In Theorem 3.1, we give the optimal parameter ω_{opt} to minimize the upper bound of the spectral radius of $\mathbf{L}(\omega)$. It holds that

$$\rho(\mathbf{L}(\omega^*)) \le \rho(\mathbf{L}(\omega_{\text{opt}})) \le \hat{\sigma}(\omega_{\text{opt}}),$$

where ω^* is the practical optimal parameter to minimize $\rho(\mathbf{L}(\omega))$. In the actual implementation, we use ω_{opt} as the theoretical optimal parameter. In the next section, we get the practical optimal parameter ω^* experimentally with line search. We will compare the numerical behavior of PMHSS with these two parameters by numerical experiments.

Remark 3.2. To simplify the process of choosing of the optimal parameter, we can choose $\hat{\omega}$ to minimize a coarse upper bound of $\rho(L(\omega))$, saying,

$$\max_{1\le j\le n} f(\lambda_j) = \frac{\sqrt{1+\lambda_j^2}}{1+\lambda_j}, \quad \text{or} \quad \max_{1\le j\le n} f(\mu_j) = \max_{1\le j\le n} \frac{\sqrt{1+\mu_j^2}}{1+\mu_j},$$

alternatively. Consequently, we have that $\max_j(f(\lambda_j(\omega)))$ obtains its minimum at

$$\omega_{\text{opt}} = \omega_1,$$

and

$$\min_{\omega} \max_{j}(f(\lambda_j(\omega))) = f(\lambda_{\max}(\omega_1)) = f(\lambda_{\min}(\omega_1));$$

while $\max_j(f\mu_j(\omega))$ obtains its minimum at

$$\omega_{\text{opt}} = \omega_2,$$

and

$$\min_{\omega} \max_{j}(f(\mu_j(\omega))) = f(\mu_{\max}(\omega_2)) = f(\mu_{\min}(\omega_2)).$$

4. Numerical experiments

In this section, we perform PMHSS iteration method, PMHSS preconditioned GMRES method, HSS-like iteration method [5] and HSS-like preconditioned GMRES method [5] to solve the linear systems arising from two fractional nonlinear Schrödinger equations. We compare the numerical performance of these methods in terms of the number of iterations (denoted by 'IT') and elapsed CPU time (denoted by 'CPU'). In this section, the theoretical optimal parameter of PMHSS iteration method (denoted by 'ω_{opt}') is calculated by Theorem 3.1. In addition, the experimental optimal parameters of PMHSS iteration method which minimize the iterative counters, (denoted by 'ω^*') is sought in $(0,\ 3]$ with step size 0.1 while the experimental optimal parameters of HSS-like iteration method (denoted by '$\widetilde{\omega}^*$') is sought in the interval $(0,\ 1]$ with the step size 0.001. In PMHSS preconditioned GMRES method (denoted by 'PMHSS-GMRES'), we fix $\omega = 1$ in PMHSS preconditioner $\mathbf{F}(\omega)$. In HSS-like preconditioned GMRES method (denoted by 'HSS-like-GMRES'), the preconditioner is defined in [5] as

$$P_{\text{hss-like}} = \frac{1}{2\tilde{\alpha}}(\tilde{\alpha}I + T)(\tilde{\alpha}I + D + \mathrm{i}I),$$

with the experimental optimal parameters.

In all numerical experiments, the initial vector is set to be the zero vector and the iterations are terminated if the current iterations satisfy $\|r_k\|_2/\|r_0\|_2 < 10^{-6}$, where r_k is the residual vector of the kth iteration and r_0 is the initial residual vector. In all the tested methods, we solve the Toeplitz linear systems by preconditioned CG method with Tony Chan's preconditioner in [24].

Example 4.1. Let $\gamma = 1,\ \rho = 2,\ \beta = 0,\ 1 < \alpha < 2.$

$$iu_t + (-\Delta)^{\frac{\alpha}{2}} u + 2|u|^2 u = 0, \quad -20 \le x \le 20,\ 0 < t \le 2, \tag{4.1}$$

subjected to the initial boundary value conditions

$$u(x,0) = \text{sech}(x)\cdot e^{2ix},\ u(-20,t) = u(20,t) = 0. \tag{4.2}$$

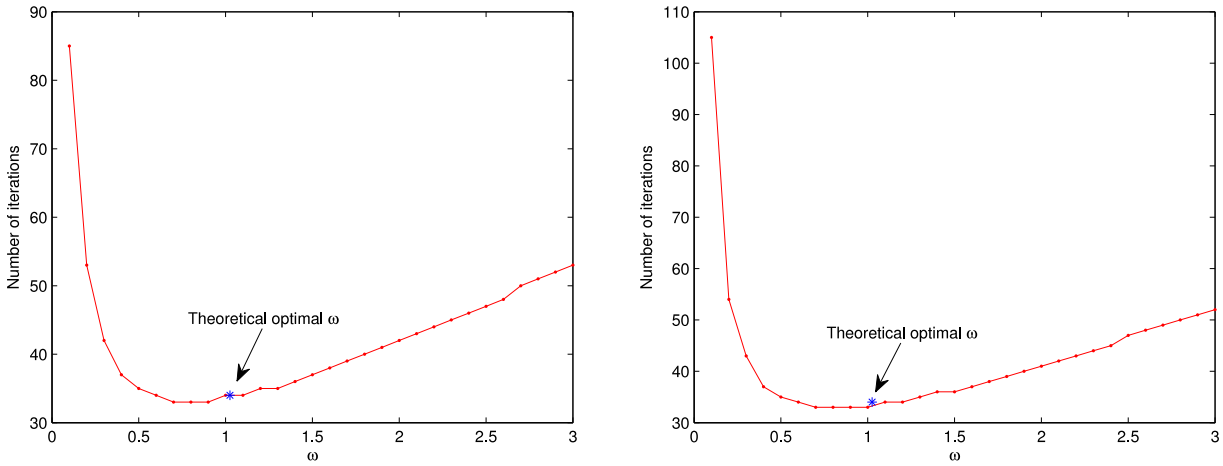

Fig. 1. The curves of IT versus ω for PMHSS iteration method when $\alpha = 1.2$ (left) and $\alpha = 1.7$ (right) for Example 4.1 when $m = 800$.

Table 1
The optimal parameters in Example 4.1 when $\alpha = 1.2$.

m	800	1600	3200	6400
ω_{opt}	1.025	1.025	1.025	1.025
ω^*	[0.8, 0.9]	[0.8, 0.9]	[0.8,1.1]	[0.8, 1.1]
$\widetilde{\omega}^*$	0.007	0.006	0.004	0.003

Table 2
The optimal parameters in Example 4.1 when $\alpha = 1.7$.

m	800	1600	3200	6400
ω_{opt}	1.025	1.025	1.025	1.025
ω^*	[0.8,1.0]	[0.8,1.0]	[0.8,1.0]	0.8
$\widetilde{\omega}^*$	0.01	0.009	0.008	0.007

In Fig. 1, we plot the curves of the iterative counters of PMHSS iteration method versus different ω when the number of the spatial discrete points m is 800. The blue star labels the iterative counter of PMHSS with the ω_{opt} theoretical optimal parameter calculated by the formula in Theorem 3.1; The dotted line labels the iterative counters of PMHSS with the ω in different test points. The plot demonstrates that PMHSS iteration method with ω_{opt} uses a few more iterations than that with experimental optimal parameter ω^*.

In Tables 1 and 2, we list the theoretical optimal parameters, experimental optimal parameters for PMHSS iteration method and the experimental optimal parameters for HSS-like iteration method for the linear systems with different scales. The optimal parameters calculated in Theorem 3.1 are very close to or included in the intervals contain the experimental optimal parameters. The optimal parameters of PMHSS iteration method are close to 1 while that of HSS-like iteration method are tend to 0 with the refined mesh. It indicates that $\omega = 1$ should be a good estimator of optimal parameters in practical choice. In addition, both ω_{opt} and ω^* are independent of not only the scale of the problems but also the fractional differential order α.

In Fig. 2, we plot the curves of the spectral radius $\rho(\mathbf{L}(\omega))$ of iteration matrix and the upper bound $\hat{\sigma}(\omega)$ for versus ω in the case of different fractional differential parameters α. It demonstrates that $\hat{\sigma}(\omega)$ approximates $\rho(\mathbf{L}(\omega))$ closely, especially when $\omega \geq 1$. Therefore, ω_{opt} which minimizes $\hat{\sigma}(\omega)$ is a reliable and proper approximation for the optimal parameter to minimizing $\rho(\mathbf{L}(\omega))$.

In Tables 3 and 4, the number of iterations and the CPU time are reported for each tested methods when $\alpha = 1.2$ and 1.7 for Example 4.1. It is shown that the theoretical optimal parameters and experimental optimal parameters yield the similar performance. The PMHSS iteration method outperforms HSS-like method in terms of both the number of iterations and the CPU time. PMHSS-GMRES method is more efficient than two iteration methods when $\alpha = 1.2$. The PMHSS-GMRES method is the most efficient method. The iterative counters of PMHSS preconditioned GMRES method and PMHSS iteration method are all independent of either the mesh size or the parameter α.

In Fig. 3, we draw the iteration history of the relative residual for the tested methods for Example 4.1 with $m = 800$, when $\alpha = 1.2$ and 1.7 respectively. It is clear that, preconditioned GMRES methods with PMHSS preconditioner is the fastest method among all the tested method. The curves of PMHSS iteration methods with parameters ω_{opt} and ω^* are almost overlapped since they have the similar convergent performance.

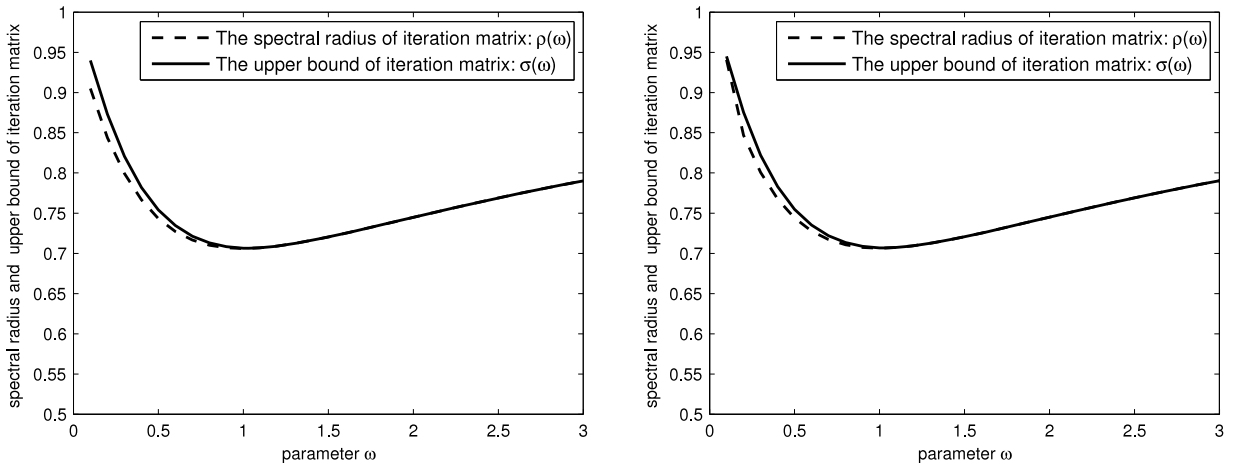

Fig. 2. The spectral radius $\rho(\mathbf{L}(\omega))$ of iteration matrix and the upper bound $\hat{\sigma}(\omega)$ for different ω when $\alpha = 1.2$ (left) and $\alpha = 1.7$ (right) for Example 4.1.

Table 3
Numerical results for Example 4.1 when $\alpha = 1.2$.

m	800		1600		3200		6400	
	IT	CPU	IT	CPU	IT	CPU	IT	CPU
PMHSS(ω_{opt})	34	4.44e−1	34	1.11	34	4.11	35	1.54e+1
PMHSS(ω^*)	33	4.08e−1	33	1.08	34	4.18	35	1.53e+1
HSS-like($\widetilde{\omega}^*$)	127	1.97	165	7.45	216	4.06e+1	280	2.01e+2
PMHSS-GMRES	13	1.96e−1	13	4.65e−1	13	1.89	13	5.99
HSS-like-GMRES	36	4.88e−1	39	4.22	44	7.24e+1	50	7.19e+2

Table 4
Numerical results for Example 4.1 when $\alpha = 1.7$.

m	800		1600		3200		6400	
	IT	CPU	IT	CPU	IT	CPU	IT	CPU
PMHSS(ω_{opt})	33	4.38e−1	33	1.15	33	4.18	34	1.50e+1
PMHSS(ω^*)	33	5.20e−1	33	1.16	33	4.22	33	1.45e+1
HSS-like($\widetilde{\omega}^*$)	256	4.05	278	1.33e+1	303	5.77e+1	357	2.54e+2
PMHSS-GMRES	15	2.22e−1	15	5.90e−1	15	1.97	15	6.61
HSS-like-GMRES	50	7.03e−1	51	1.83	53	1.99e+1	56	3.33e+2

Example 4.2. For the following coupled system with $\gamma = 1,\ \rho = 2,\ \beta = 1,\ 1 < \alpha < 2$.

$$\begin{cases} iu_t + (-\Delta)^{\frac{\alpha}{2}} u + 2(|u|^2 + |v|^2)u = 0, \\ iv_t + (-\Delta)^{\frac{\alpha}{2}} v + 2(|v|^2 + |u|^2)v = 0, \end{cases} \quad -20 \le x \le 20,\ 0 < t \le 2, \tag{4.3}$$

we take the initial boundary value conditions of the form

$$\begin{aligned} &u(x,0) = \operatorname{sech}(x+1)\cdot\exp(2ix),\ \ v(x,0) = \operatorname{sech}(x-1)\cdot\exp(-2ix), \\ &u(-20,t) = u(20,t) = 0,\ \ v(-20,t) = v(20,t) = 0. \end{aligned} \tag{4.4}$$

This is a coupled fractional nonlinear Schrödinger equations. In every temporal step, we solve two Toeplitz-like system of equations. In Table 5, we report the theoretical optimal parameters and the experimental optimal parameters of the PMHSS iteration method, as well as the experimental optimal parameters of the HSS-like iteration method when $\alpha = 1.2$ and 1.7 for Example 4.2. ω_u and is the parameter for the linear system of u while ω_v is the parameter for linear system of v.

It is observed that the optimal parameters of the PMHSS iteration method are nearly around 1, which are independent of the mesh size. This is similar with the result in Example 4.1. On the other hand, the experimental optimal parameters of the HSS-like iteration method is very small, which is independent of not only the mesh size, but also the fractional differential parameter α. In Tables 6 and 7, numerical results including in the number of iteration steps and the CPU time are reported for the tested methods.

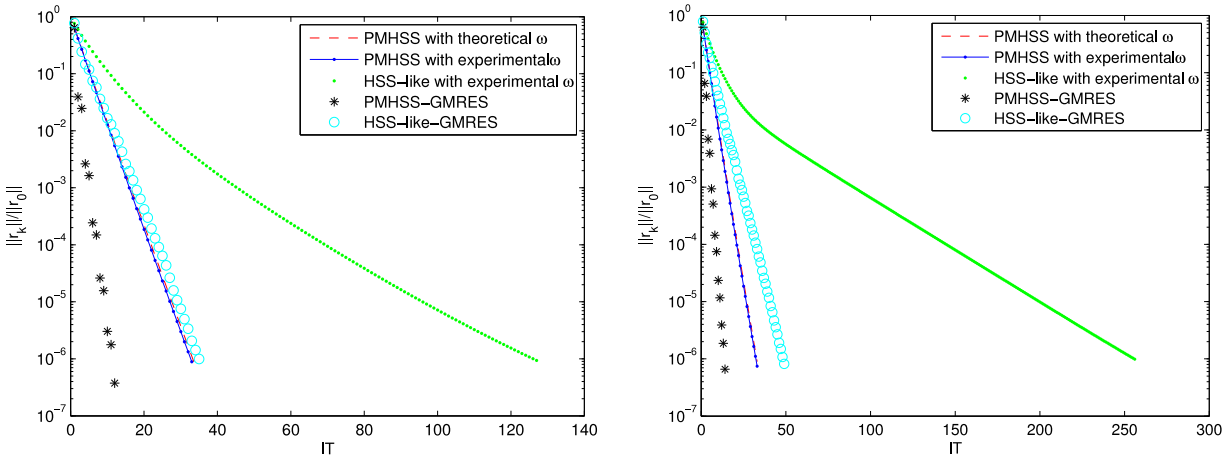

Fig. 3. The curves of the relative residual versus the iteration steps for Example 4.1 when $\alpha = 1.2$ (left) and $\alpha = 1.7$ (right).

Table 5
The optimal parameters for Example 4.2.

α		1.2			1.7		
m		1600	3200	6400	1600	3200	6400
ω_{opt}	ω_u	1.0135	1.0135	1.0135	1.0135	1.0135	1.0135
	ω_v	1.0276	1.0276	1.0276	1.0279	1.0279	1.0279
ω^*	ω_u	[0.7, 0.9]	[0.6, 0.9]	[0.7, 1.0]	[0.6, 1.0]	[0.7, 1.0]	[0.7, 0.9]
	ω_v	[0.7, 0.9]	[0.6, 0.9]	[0.7, 1.0]	[0.6, 1.0]	[0.7, 1.0]	[0.7, 0.9]
$\widetilde{\omega}^*$	ω_u	0.006	0.004	0.003	0.009	0.008	0.007
	ω_v	0.006	0.004	0.003	0.009	0.008	0.007

Table 6
Numerical results for Example 4.2 when $\alpha = 1.2$.

m	1600		3200		6400		12 800	
	IT	CPU	IT	CPU	IT	CPU	IT	CPU
PMHSS(ω_{opt})	33	2.62	33	8.48	34	3.23e+1	35	1.08e+2
PMHSS(ω^*)	32	2.42	33	8.65	34	3.23e+1	35	1.05e+2
HSS-like($\widetilde{\omega}^*$)	166	1.81e+1	224*	9.05e+1	289*	4.37e+2	414	1.49e+3
PMHSS-GMRES	13	1.02	13	3.63	13	1.23e+1	13	3.92e+1
HSS-like-GMRES	11	7.28e−1	11	2.72	11	1.04e+1	11	2.63e+1

Table 7
Numerical results for Example 4.2 when $\alpha = 1.7$.

m	1600		3200		6400		12 800	
	IT	CPU	IT	CPU	IT	CPU	IT	CPU
PMHSS(ω_{opt})	32	2.65	32	8.81	33	3.15e+1	33	9.66e+1
PMHSS(ω^*)	32	2.52	32	8.83	32	3.04e+1	33	9.96e+1
HSS-like($\widetilde{\omega}^*$)	281*	3.25e+1	308*	1.26e+2	340*	5.26e+2	397*	1.38e+3
PMHSS-GMRES	15	1.28	15	4.29	15	1.53e+1	15	4.68e+1
HSS-like-GMRES	15	1.08	15	3.88	15	3.38e+1	15	3.62e+2

According to the listed data in Tables 6 and 7, HSS-like preconditioned GMRES method is the fastest method when $\alpha = 1.2$, while PMHSS preconditioned GMRES method is the fastest one for large scale problems when $\alpha = 1.7$. For all listed methods, we report only one value of IT in each case, even though we solve two linear systems of equations with u and v. Actually, except for HSS-like iteration, all the methods find the satisfactory u and v in the same numbers of iterative steps. However, the iterative counter of HSS-like for solving u are a slight different with that for solving v. We label $*$ on the corresponding data. A notable phenomenon is that even with the similar numbers of iterative

steps, HSS-like preconditioned GMRES method takes much more CPU time than PMHSS preconditioned GMRES method, especially, when $m = 6400$ or $m = 12\,800$ and $\alpha = 1.7$. The primary reason is HSS-like method contains complex value arithmetics, therefore, it generates the complex sequence. The operation of complex value arithmetics is much more expensive than that of real value arithmetics. In every iteration, HSS-like preconditioned GMRES method solves a linear system with $\tilde{\omega}I + T$. Even though the coefficient matrix is symmetric positive definite, the right hand side vector is complex. The complex version preconditioned CG method is performed. Thus when the problem size becomes larger, the complex arithmetics in preconditioned GMRES method with HSS-like preconditioner are more consuming. Also, the PMHSS iteration method outperforms HSS-like method considerably in terms of the number of iterations and CPU time. The PMHSS iteration method is still independently of not only the mesh size but also the fractional differential parameter.

5. Conclusion

A preconditioned modified Hermitian and skew-Hermitian splitting iteration method is proposed for the discrete space fractional coupled nonlinear Schrödinger equations by taking advantage of the Toeplitz structure of the coefficient matrix. We characterize the optimal parameters for the iteration scheme by writing the upper bound of the spectral radius piecewise explicitly. The numerical experiments show that the achieved parameter is very close to the optimal parameter for minimizing the spectral radius. The iteration method yields an efficient preconditioner also. Both PMHSS iteration method and the PMHSS preconditioned GMRES method are effective and efficient for solving the Toeplitz-like complex linear system arising from the discrete space fractional nonlinear Schrödinger equations. The numerical results indicate that the convergence of these methods are independent of both the mesh size of the discretization and the fractional differential parameter.

References

[1] N. Laskin, Fractional quantum mechanics and Lévy path integrals, Phys. Lett. A 268 (4) (2000) 298–305.
[2] X.-Y. Guo, M.-Y. Xu, Some physical applications of fractional Schrödinger equation, J. Math. Phys. 47 (8) (2006) 82–104.
[3] B.-L. Guo, Y.-Q. Han, J. Xin, Existence of the global smooth solution to the period boundary value problem of fractional nonlinear Schrödinger equation, Appl. Math. Comput. 204 (1) (2008) 468–477.
[4] J.-Q. Hu, J. Xin, H. Lu, The global solution for a class of systems of fractional nonlinear Schrödinger equations with periodic boundary condition, Comput. Math. Appl. 62 (3) (2011) 1510–1521.
[5] Y.-H. Ran, J.-G. Wang, D.-L. Wang, On HSS-like iteration method for the space fractional coupled nonlinear SchröDinger equations, Appl. Math. Comput. 271 (2015) 482–488, http://dx.doi.org/10.1016/j.amc.2015.09.028.
[6] Y.-H. Ran, J.-G. Wang, D.-L. Wang, On preconditioners based on HSS for the space fractional CNLS equations, East Asian J. Appl. Math. 7 (1) (2017) 70–81.
[7] D.-L. Wang, A.-G. Xiao, W. Yang, Crank–nicolson difference scheme for the coupled nonlinear Schrödinger equations with the Riesz space fractional derivative, J. Comput. Phys. 242 (2013) 670–681.
[8] D.-L. Wang, A.-G. Xiao, W. Yang, A linearly implicit conservative difference scheme for the space fractional coupled nonlinear Schrödinger equations, J. Comput. Phys. 272 (2014) 644–655.
[9] D.-L. Wang, A.-G. Xiao, W. Yang, Maximum-norm error analysis of a difference scheme for the space fractional CNLS, Appl. Math. Comput. 257 (2015) 241–251.
[10] L. Gauckler, C. Lubich, Nonlinear Schrödinger equations and their spectral semi-discretizations over long times, Found. Comput. Math. 10 (2) (2010) 141–169.
[11] J.-Q. Sun, M.-Z. Qin, Multi-symplectic methods for the coupled 1D nonlinear Schrödinger system, Comput. Phys. Comm. 155 (3) (2003) 221–235.
[12] A. Aydin, B. Karasoezen, Multi-symplectic integration of coupled non-linear Schrödinger system with soliton solutions, Int. J. Comput. Math. 86 (5) (2009) 864–882.
[13] Z.-Z. Sun, D.-D. Zhao, On the L_∞ convergence of a difference scheme for coupled nonlinear Schrödinger equations, Comput. Math. Appl. 59 (10) (2010) 3286–3300.
[14] M.K. Ng, J. Pan, Approximate inverse circulant-plus-diagonal preconditioners for Toeplitz-plus-diagonal matrices, SIAM J. Sci. Comput. 32 (3) (2010) 1442–1464.
[15] S.-L. Lei, H.-W. Sun, A circulant preconditioner for fractional diffusion equations, J. Comput. Phys. 242 (2013) 715–725.
[16] J.-Y. Pan, R.-H. Ke, M.K. Ng, H.-W. Sun, Preconditioning techniques for diagonal-times-Toeplitz matrices in fractional diffusion equations, SIAM J. Sci. Comput. 36 (6) (2014) 2698–2719.
[17] T. Chan, An optimal circulant preconditioner for Toeplitz systems, SIAM J. Sci. Stat. Comput. 9 (1988) 766–771.
[18] R. Chan, G. Strang, Toeplitz equations by conjugate gradients with circulant preconditioner, SIAM J. Sci. Stat. Comput. 10 (1989) 104–119.
[19] R. Chan, M.K. Ng, Conjugate gradient methods for toeplitz systems, SIAM Rev. 38 (1996) 427–482.
[20] Z.-Z. Bai, G.H. Golub, M.K. Ng, Hermitian and skew-hermitian splitting methods for non-hermitian positive definite linear systems, SIAM J. Matrix Anal. Appl. 24 (3) (2003) 603–626.
[21] Y.-H. Ran, J.-G. Wang, D.-L. Wang, On partially inexact HSS iteration methods for the complex symmetric linear systems in space fractional CNLS equations, J. Comput. Appl. Math. 317 (3) (2017) 128–136, http://dx.doi.org/10.1016/j.cam.2016.11.030.
[22] Z.-Z. Bai, On preconditioned iteration methods for complex linear systems, J. Engrg. Math. 93 (1) (2015) 41–60.
[23] Z.-Z. Bai, M. Benzi, F. Chen, Z.-Q. Wang, Preconditioned MHSS iteration methods for a class of block two-by-two linear systems with applications to distributed control problems, IMA J. Numer. Anal. 33 (1) (2013) 343–369.
[24] R. Chan, X.-Q. Jin, An Introduction to Iterative Toeplitz Solvers, SIAM, Philadelphia, 2007.